Intersubband absorption of cubic GaN/Al(Ga)N quantum wells in the near-infrared to terahertz spectral range

H. Machhadani,[1] M. Tchernycheva,[1,*] S. Sakr,[1] L. Rigutti,[1] R. Colombelli,[1] E. Warde,[1] C. Mietze,[2] D. J. As,[2] and F. H. Julien[1]

[1]*Institut d'Electronique Fondamentale, UMR 8622 CNRS, University Paris-Sud 11, F-91405 Orsay, France*

[2]*Department of Physics, University of Paderborn, Warburger Strasse 100, D-33095 Paderborn, Germany*

(Received 20 October 2010; revised manuscript received 7 January 2011; published 23 February 2011)

The intersubband absorption of cubic GaN/Al(Ga)N quantum wells is studied experimentally and theoretically over a wide spectral range. By changing the quantum well thickness it is possible to tune the intersubband absorption peak wavelength from 1.4 μm (214 THz) to 63 μm (4.76 THz). Comparing the experimental results with simulations based on the effective-mass model we demonstrate that the GaN/AlN conduction-band offset is higher than 1.2 eV. The best fit with the experimental data is achieved for a conduction-band offset of 1.4 eV and for a GaN effective mass of $0.11m_0$.

DOI: 10.1103/PhysRevB.83.075313 PACS number(s): 78.67.De, 81.07.St, 78.30.Fs

I. INTRODUCTION

Thanks to recent advances in material growth and fabrication technologies, GaN/AlN superlattices have become the system of choice for intersubband (ISB) devices operating at telecommunication wavelengths,[1,2] such as, for example, fast photodetectors[3,4] or modulators.[5,6] Recently it has been predicted that because of the large optical phonon energy in nitride-based semiconductors, these materials are very promising candidates for ISB lasers emitting in the THz domain with room-temperature operation.[7]

The stable phase for nitride crystals is the hexagonal phase, which is characterized by the presence of spontaneous and piezoelectric polarizations along the *c* axis. For thin-film heterostructures the polarization discontinuity at the interfaces results in a strong internal electric field in the layers.[8] In case of interband devices, this field separates electrons and holes, reducing the luminescence efficiency of light-emitting diodes. It also distorts the potential and leads to carrier accumulation regions.[1] For ISB devices, the internal field not only complicates the design, but it also prevents tuning the ISB absorption into the far-infrared range of electromagnetic spectrum. Indeed, for large GaN/AlN quantum wells (QWs) the internal field confines carriers in the triangular potential, independent of the QW width. Mid-IR ISB absorptions up to 10 μm have been reported in large GaN/Al(Ga)N hexagonal QWs,[9] but further reduction of the internal electric field is needed in order to cover the THz spectral domain. The problem of the internal electric field related to the polar nature of wurtzite crystals has motivated the development of the zinc-blende nitride materials. The LO phonon energy in cubic GaN is almost the same as in wurtzite GaN [92.7 meV (Ref. 10)], whereas the effective mass is much smaller. The electron effective mass in cubic GaN is in the range $0.11m_0$–$0.17m_0$ (Refs. 11 and 12) as compared to $0.2m_0$ in wurtzite GaN.[13] A lower effective mass would result in a higher gain and lower threshold current density in quantum cascade lasers.[14]

Zinc-blende GaN, InN, and AlN epilayers have been synthesized successfully using plasma-assisted molecular-beam epitaxy (PA-MBE).[15] Recently freestanding GaN substrates also have been produced.[16] The ISB absorptions in cubic GaN/AlN QWs have been observed in the near-infrared spectral range[17] and a near-infrared QW photodetector (QWIP) has been demonstrated.[18] Resonant tunneling in cubic GaN/AlGaN double-barrier structures has also been reported.[19] However, no study of the ISB transitions in the mid- and far-infrared spectral ranges in cubic nitride superlattices has been reported so far.

In this paper we study the ISB absorptions of cubic GaN/Al(Ga)N QW superlattices over a wide spectral range. We show that by changing the QW thickness and Al content it is possible to tune the ISB absorption wavelength from 1.4 μm (214 THz) to 63 μm (4.76 THz). To the best of our knowledge, these values correspond respectively to the shortest and the longest wavelengths for ISB transitions ever achieved in this material system. Comparing the experimental results with simulations based on the effective-mass model, we show that the conduction-band offset (CBO) between GaN and AlN is higher than 1.2 eV. The best fit with the experimental data is achieved for a CBO of 1.4 eV and a GaN effective mass of $0.11m_0$.

II. SAMPLE DESCRIPTION AND CHARACTERIZATION

The samples were grown by PA-MBE on a 10-μm-thick 3C-SiC on Si(001) templates. This substrate has been chosen owing to its good transparency both in the near infrared and in the far-infrared spectral range. All quantum structures were grown at $T_{\text{substrate}} = 720\,^{\circ}\text{C}$. The growth was controlled by *in situ* reflection high-energy electron diffraction (RHEED). The GaN layers were grown under 1 monolayer (ML) Ga coverage, which was found to be the optimal growth condition for cubic GaN,[20] while the AlN layers were grown under N-rich conditions.[21] The growth of the superlattice was interrupted after each layer to evaporate excess metal from the surface. The thickness of the AlN layers was controlled by RHEED-intensity oscillations while the GaN growth rate was estimated from AlGaN growth oscillations and thickness measurements on the reference sample. The growth rate for AlN and GaN were 0.19 and 0.18 ML/s, respectively. More details on the growth can be found in Ref. 15.

The samples consist of a 100-nm-thick GaN buffer layer followed by 40 periods of GaN/Al(Ga)N QWs and a GaN cap layer. The cap layer thickness is 7 nm for samples A, B, and C and 30 nm for sample D. The QWs are *n* doped with Si in order to populate the ground electronic state. The QW thickness is varied in order to tune the ISB fundamental e_1–e_2 transition

TABLE I. Structural and optical parameters for GaN/Al(Ga)N QW Sample.

Sample	QW thickness (nm)	Barrier thickness (nm)	Al content in the barriers(%)	Doping in the QWs (cm^{-3})	PL energy (eV) [FWHM (eV)]	ISB energy (eV) [FWHM (eV)]
A	2	3	100	5×10^{19}	3.67(0.267)	0.882(0.170)
B	3	3	100	1×10^{19}	3.43(0.149)	0.46(0.180)
C	5	3	100	1×10^{19}	3.32(0.13)	0.304(0.2)
D	12	15	5	2×10^{17}	3.21(0.051)	0.0197(0.009)

energy. The QW and barrier thicknesses and the doping level are summarized in Table I.

The structural quality of the GaN/Al(Ga)N superlattices was assessed using x-ray diffraction. From the positions of additional satellites in the ω-2θ scans of the symmetrical (002) reflection, the lattice period of the superlattice structures was inferred. In addition, simulations for the x-ray measurements were performed using a dynamical scattering theory.[22] By using x-ray simulations, not only the lattice parameter but also the thicknesses of the individual layers can be determined. Good agreement between the experimental and calculated data can be achieved only by assuming the correct thicknesses for both the QW and barrier layers. Figure 1 shows an example of a ω-2θ scan of sample B with the related simulation. The layer thicknesses deduced from x-ray diffraction for all samples are in good agreement with the nominal ones. In addition, the strain in the superlattice samples was investigated by reciprocal space maps of the asymmetrical (113) reflection. For samples A, B, and C we find that the AlN layers are not fully strained on GaN. From the position of the superlattice reflections we conclude that the superlattice structure has formed an average lattice constant between GaN and AlN, meaning that the AlN layers are partially relaxed while the GaN is partially strained.

The samples were then characterized by UV photoluminescence (PL) spectroscopy. The excitation is provided with a continuous-wave frequency-doubled Ar^{2+} laser ($\lambda = 244$ nm) and the spectra are analyzed using a Jobin Yvon HR460 spectrometer equipped with a liquid-nitrogen-cooled CCD camera. The room-temperature PL spectra of the four samples are shown in Fig. 2. The emission energy (summarized in Table I) progressively redshifts with increasing QW thickness. For cubic nitrides no internal field is expected in the QWs. Indeed, the measured energies are in good agreement with calculations performed assuming a rectangular potential profile (cf. Fig. 4 and the corresponding discussion).

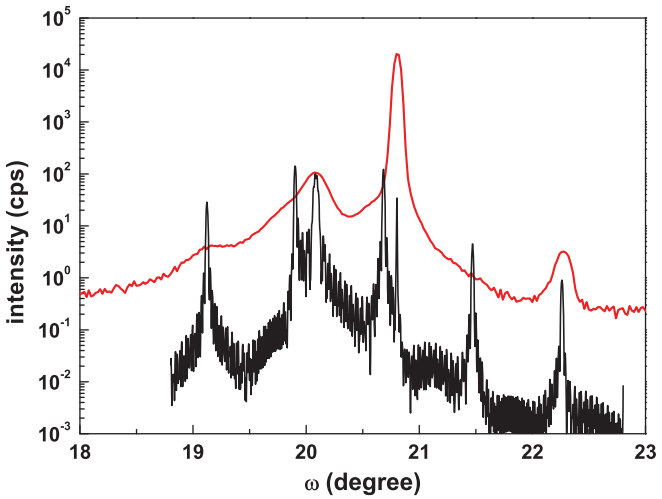

FIG. 1. (Color online) X-ray diffraction ω-2θ spectrum of sample B (top curve) and a corresponding simulation with nominal layer thicknesses (bottom curve).

III. INTERSUBBAND ABSORPTION IN GaN/AlN QWs IN THE NEAR- AND MIDINFRARED SPECTRAL RANGE

For ISB absorption measurements, the samples were polished in a multipass waveguide geometry with parallel facets tilted by 30° with respect to the substrate plane. The 30° angle is chosen in order to avoid both the total internal reflection on the Si/SiC interface ($\theta_{\text{critical}} \sim 48°$) and to maximize the interaction of the electromagnetic field with the dipole of the ISB transition (which is oriented along the growth axis). The sample length corresponds to ~14 passes through the active region. Infrared absorption measurements were performed at room temperature using a Fourier transform infrared spectrometer. A typical transmission spectrum for TM- (*p*-) and TE- (*s*-) polarized light is shown in the inset to Fig. 3. The spectrum is normalized by the transmission

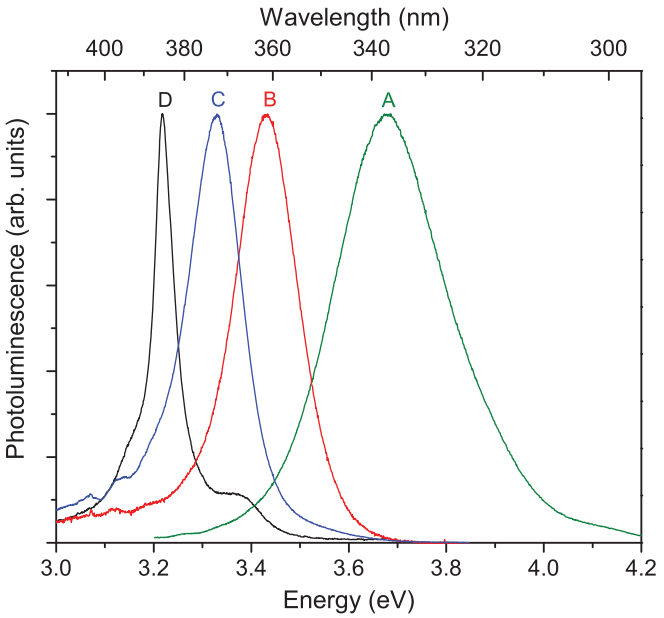

FIG. 2. (Color online) Room-temperature PL spectra of the four studied samples.

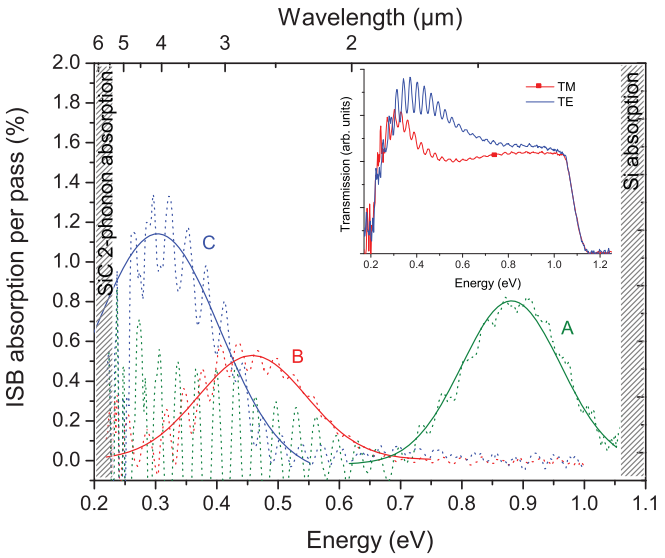

FIG. 3. (Color online) Room-temperature TM absorption (characteristic of ISB transitions) per pass in the active region of samples A, B, and C (dotted curves) and corresponding Gaussian fits (full curves). Inset: Room-temperature infrared transmission spectrum of sample B for TM- and TE-polarized light.

of a reference sample (600-nm-thick cubic GaN epilayer on SiC on silicon). The oscillations observed in the spectrum arise from Fabry-Pérot interferences in the 10-μm-thick SiC layer. The high-energy cutoff corresponds to the absorption of the Si substrate whereas the low-energy transmission drop at 0.21 eV corresponds to the two-phonon absorption of the SiC template.[23] An absorption peaked at 0.46 eV is observed for TM-polarized light. The TM polarization is a signature of an ISB resonance.

Figure 3 displays the ISB absorption spectra of samples A, B, and C together with the corresponding Gaussian fits. The spectra are corrected for the baseline and normalized by the number of passes through the active region. The absorptions are peaked at $\lambda = 1.4$, 2.7, and 4.1 μm for samples A, B, and C, respectively.

The broadening of the ISB absorption in the present cubic QW samples is larger than the values typically observed in their hexagonal counterparts. For example, for sample A the full width at half maximum (FWHM) is 0.17 eV, which is slightly higher than the typical broadening observed for hexagonal GaN/AlN QWs with absorption in the same spectral range (typically FWHM = 60–100 meV in doped QWs[24,25] and 40 meV in undoped samples[26]). It should be noted also that for cubic QWs the ISB absorption resonance can be well fitted by a Gaussian function contrary to the wurtzite QWs where the absorption follows a Lorentzian or a multi-Lorentzian shape.[25] This suggests that the broadening of the ISB transitions in cubic QWs originates from thickness fluctuations and interface roughness, as is the case for GaAs/AlGaAs QWs.[27]

IV. MODELING OF THE QUANTUM CONFINEMENT

The quantum confinement in cubic QWs was modeled using an effective-mass approximation. The PL and ISB transition energies of the investigated structures were calculated by self-consistently solving the Schrödinger and Poisson equations, assuming sharp interfaces. The nonparabolicity of the conduction band of GaN was neglected. In the literature, a large dispersion of material parameters for cubic GaN and AlN is reported. In particular, the effective masses and the band offsets are not well known. For the effective masses, we have used three parameter sets deduced from Ref. 11 (empirical pseudopotential calculations) and Refs. 12 and 28 (full potential linear augmented plane-wave method). The effective-mass values are summarized in Table II. As for the band offsets, there are mainly theoretical studies that suggest valence-band offset (VBO) values in the 0.4–1.36 eV range (a review can be found in Ref. 13). For instance, the first-principle calculations of Ref. 29 predict a type-I band alignment and a GaN/AlN VBO of 0.98 eV for pseudomorphic growth on an AlN substrate, and 0.63 eV for growth on a GaN substrate. Taking into account the uncertainty in the reported values of the band gap of cubic AlN [3.9 eV–6.7 eV (Ref. 30)], this results in an even larger dispersion of the CBO values. (It should be noted that the relevant parameter to calculate the CB offset is the AlN band gap at the Γ point and not the indirect band gap at the X point.) An empirical rule of 70:30 for the CBO-VBO ratio is also used,[17] yielding $\sim$1.33 eV for the CBO. In our calculations the CBO is considered as a fitting parameter.

TABLE II. Effective masses for electronic and heavy hole bands in cubic GaN and AlN from Refs. 11, 12, and 28.

Reference	m_e^*GaN	m_{hh}^*GaN	m_e^*AlN	m_{hh}^*AlN
11	$0.11m_0$	$0.8m_0$	$0.19m_0$	$1.2m_0$
28	$0.14m_0$	$0.86m_0$	$0.28m_0$	$1.44m_0$
12	$0.17m_0$	$0.85m_0$	$0.3m_0$	$1.39m_0$

Figure 4 shows the simulation results for PL and ISB transition energies calculated with different effective-mass sets from Refs. 11, 12, and 28 and a CBO of 1.2 eV. The simulations are compared with the experimental data. The PL peak energy is almost band offset independent, but it is strongly sensitive to the effective masses. Figure 4 (top panel) shows that the theory-experiment agreement improves when the effective mass decreases. The best fit is achieved for the smallest electronic effective mass in GaN, $m_e^* = 0.11m_0$.[11] This effective-mass value also yields a good agreement with the experimental ISB absorption energies (Fig. 4, bottom panel).

It is important to note that the observation of an ISB peak energy as high as 0.882 eV allows us to draw a conclusion about the CBO value. Indeed, calculations for different offset values and different effective-mass sets demonstrate that the minimal CBO necessary to sustain an electronic transition of 0.882 eV is 1.2 eV, regardless of the effective mass and the QW thickness used. In Fig. 5, we take the effective masses from Ref. 11 (i.e., $m_e^*\text{GaN} = 0.11m_0$), we calculate the ISB transition energy for different CBO values (1, 1.2, and 1.4 eV), and we compare with the experimental data. The ISB transition energy is more sensitive to the CB offset for narrow QWs than for large QWs. The best theory-experiment agreement is achieved for a CBO of 1.4 eV.

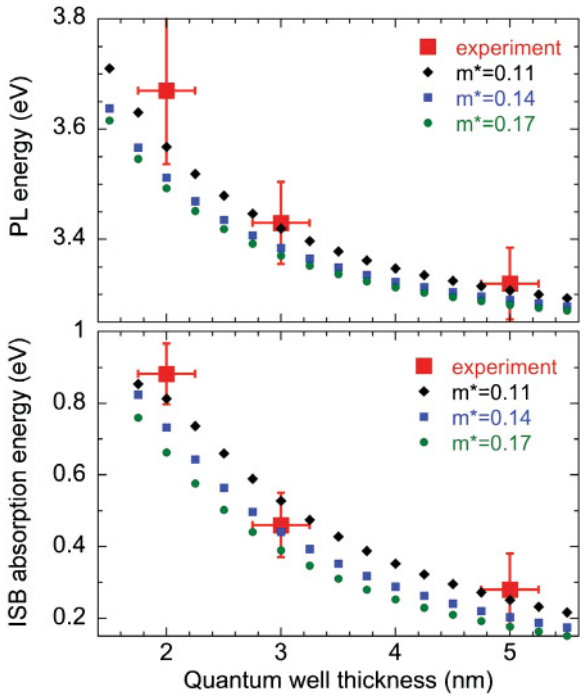

FIG. 4. (Color online) PL and ISB transition energies calculated within effective-mass approximation compared to the experimental data. The following parameters are used in the calculations : CBO = 1.2 eV for all curves; black diamonds—m_e^*GaN = $0.11m_0$, m_{hh}^*GaN = $0.8m_0$, m_e^*AlN = $0.19m_0$, m_{hh}^*AlN = $1.2m_0$; blue squares—m_e^*GaN = $0.14m_0$, m_{hh}^*GaN = $0.86m_0$, m_e^*AlN = $0.28m_0$, m_{hh}^*AlN = $1.44m_0$; green circles—m_e^*GaN = $0.17m_0$, m_{hh}^*GaN = $0.85m_0$, m_e^*AlN = $0.3m_0$, m_{hh}^*AlN = $1.39m_0$. Large red squares represent the experimental data. The error bars correspond to a ±1 ML thickness fluctuation for the abscissa and to the FWHM of the transition for the ordinate.

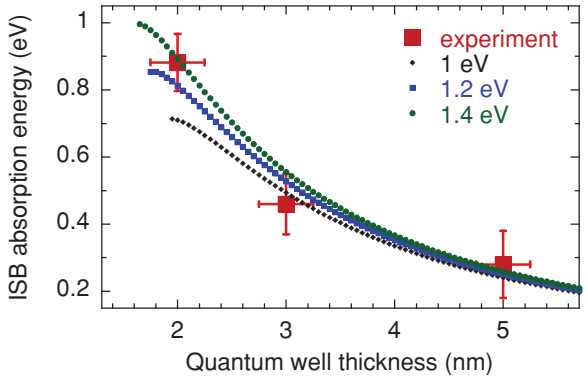

FIG. 5. (Color online) ISB absorption energies calculated for different CBO values within effective-mass approximation compared to the experimental data. Black diamonds: CBO = 1 eV. Blue squares: CBO = 1.2 eV. Green circles: CBO = 1.4 eV. The following effective masses are used: m_e^*GaN = $0.11m_0$, m_{hh}^*GaN = $0.8m_0$, m_e^*AlN = $0.19m_0$, and m_{hh}^*AlN = $1.2m_0$. Large red squares represent the experimental ISB energy. The error bars correspond to a ±1 ML thickness fluctuation for the abscissa and to the FWHM of the transition for the ordinate.

V. INTERSUBBAND ABSORPTION IN GaN/AlGaN QWs IN THE TERAHERTZ SPECTRAL RANGE

The transmission measurements in the THz spectral region were performed at a temperature of 4.7 K in a Bruker Fourier-transform infrared spectrometer equipped with a glow-bar source and a liquid-helium-cooled Si bolometer. The sample was cut into two pieces of the same length. Both pieces, after polishing the facets at a 30° angle, were placed face to face under mechanical pressure and mounted on the cold finger of a liquid-helium-cooled cryostat. This configuration allows to enhance the light transmission by doubling the surface of the input facet. Moreover, it is known that the transverse electric field is weak in the λ/n vicinity of the semiconductor-air interface (where λ is the wavelength and n is the semiconductor refractive index) because of the zero transverse electric-field boundary condition for TM-polarized light.[31] Therefore, the standard multipass waveguide configuration used for the near-infrared measurements is not optimal for the far-infrared spectral range for which λ/n is very large as compared to the active region thickness. On the contrary, placing the active QWs face to face provides a good coupling of the TM-polarized THz radiation with the ISB transitions. Two pieces of a 600-nm-thick cubic GaN epilayer on a SiC-on-silicon (001) template with approximately the same length placed face to face were used as a reference.

Figure 6 shows the transmission spectrum of sample D for TM- and TE-polarized light. The transmission of the sample has been normalized to 1 at low energies. Sample D exhibits an absorption peaked at 19.7 meV (4.76 THz) only for TM-polarized light, which is a clear signature of its ISB origin. The three unpolarized absorption resonances between 30 and 40 meV are related to the SiC-on-Si substrate. They appear only at low temperature and can be tentatively attributed to impurity absorption in SiC (shallow nitrogen donor absorption[32]).

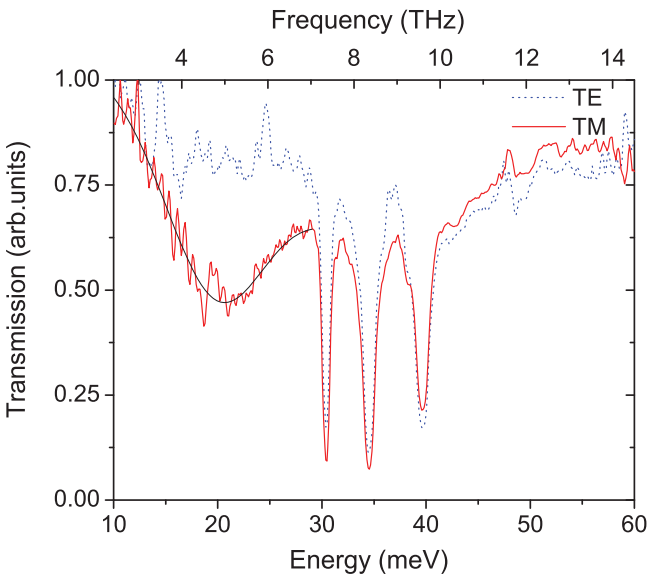

FIG. 6. (Color online) Low-temperature far-infrared transmission spectrum of sample D for TM-polarized light (red solid line) and TE-polarized light (blue dotted line). The black solid line is a Gaussian fit of the absorption with a linear baseline.

The transition energy for sample D is calculated to be 31 meV using the nominal growth thicknesses, the material parameters of Ref. 11, and taking a linear approximation for $Al_{0.05}Ga_{0.95}$ N parameters. This value is higher than the experimental ISB energy in sample D. This discrepancy may be owing to the uncertainty on the bowing parameter for the $Al_{0.05}Ga_{0.95}$ N alloy (which was taken as zero in the present calculation) or to the deviation of the actual Al content in the barriers from the nominal value. The FWHM of the ISB absorption is 9 meV, which corresponds to a relative broadening factor $\Delta\lambda/\lambda$ of 45%. This rather large broadening could be attributed to the fluctuation of the QW thickness and to the electron-impurity and electron-electron scattering.

VI. CONCLUSION

In conclusion, we have performed an experimental and theoretical study of the ISB transitions in GaN/Al(Ga)N cubic quantum wells. The ISB absorption wavelength was tuned from 1.4 μm (telecommunication range) to 63 μm (THz frequency range). To the best of our knowledge, these values correspond, respectively, to the shortest and the longest ISB wavelength achieved to date in this material system. Simulations of the quantum confinement in the framework of effective-mass approximation allow us to refine the material parameters. Namely, the electron effective mass in cubic GaN is estimated to be close to $0.11m_0$ and the CB offset between GaN and AlN is 1.2 eV or even higher. The observation of the ISB absorption at THz frequencies in GaN/$Al_{0.05}Ga_{0.95}$ N QWs opens prospects for the future development of quantum cascade lasers in this material system.

ACKNOWLEDGMENTS

The authors acknowledge financial support by the EC FET-OPEN program "Unitride" under Grant agreement ga#233950, the French National Research Agency Project "Cosni" ANR-08-BLAN-0298-01, and the German Science Foundation (DFG).

*maria.tchernycheva@u-psud.fr

[1] H. Machhadani, P. Kandaswamy, S. Sakr, A. Vardi, A. Wirtmüller, L. Nevou, F. Guillot, G. Pozzovivo, M. Tchernycheva, A. Lupu, L. Vivien, P. Crozat, E. Warde, C. Bougerol, S. Schacham, G. Strasser, G. Bahir, E. Monroy, and F. H. Julien, New J. Phys. **11**, 125023 (2009).

[2] M. Tchernycheva, L. Nevou, L. Vivien, F. H. Julien, P. K. Kandaswamy, E. Monroy, A. Vardi, and G. Bahir, Phys. Status Solidi B **247**, 1622 (2010).

[3] A. Vardi, G. Bahir, F. Guillot, C. Bougerol, E. Monroy, S. E. Schacham, M. Tchernycheva, and F. H. Julien, Appl. Phys. Lett. **92**, 011112 (2008).

[4] A. Vardi, N. Kheirodin, L. Nevou, H. Machhadani, L. Vivien, P. Crozat, M. Tchernycheva, R. Colombelli, F. H. Julien, F. Guillot, C. Bougerol, E. Monroy, S. Schacham, and G. Bahir, Appl. Phys. Lett. **93**, 193509 (2008).

[5] L. Nevou, N. Kheirodin, M. Tchernycheva, L. Meignien, P. Crozat, A. Lupu, E. Warde, F. H. Julien, G. Pozzovivo, S. Golka, G. Strasser, F. Guillot, and E. Monroy, Appl. Phys. Lett. **90**, 223511 (2007).

[6] N. Kheirodin, L. Nevou, H. Machhadani, P. Crozat, L. Vivien, M. Tchernycheva, A. Lupu, F. H. Julien, G. Pozzovivo, S. Golka, G. Strasser, F. Guillot, and E. Monroy, IEEE Photon. Technol. Lett. **20**, 724 (2008).

[7] E. Bellotti, K. Driscoll, T. D. Moustakas, and R. Paiella, Appl. Phys. Lett. **92**, 101112 (2008).

[8] F. Bernardini and V. Fiorentini, Phys. Rev. B **57**, R9427 (1998).

[9] P. K. Kandaswamy, H. Machhadani, C. Bougerol, S. Sakr, M. Tchernycheva, F. H. Julien, and E. Monroy, Appl. Phys. Lett. **95**, 141911 (2009).

[10] R. Brazis and R. Raguotis, Opt. Quantum Electron. **38**, 339 (2006).

[11] S. K. Pugh, D. J. Dugdale, S. Brand, and R. A. Abram, Semicond. Sci. Technol. **14**, 23 (1999).

[12] M. Suzuki and T. Uenoyama, Appl. Phys. Lett. **69**, 3378 (1996).

[13] I. Vurgaftman, J. R. Meyer, and L. R. Ram-Mohan, J. Appl. Phys. **89**, 5815 (2001), and references therein.

[14] L. Ajili, G. Scalari, N. Hoyler, M. Giovannini, and J. Faist, Appl. Phys. Lett. **87**, 141107 (2005).

[15] D. J. As, Microelectron. J. **40**, 204 (2009).

[16] S. V. Novikov, C. T. Foxon, and A. J. Kent, Phys. Status Solidi A **207**, 1277 (2010).

[17] E. A. DeCuir, E. Fred, M. O. Manasreh, J. Schörmann, D. J. As, and K. Lischka, Appl. Phys. Lett. **91**, 041911 (2007).

[18] E. A. DeCuir, M. O. Manasreh, E. Tschumak, J. Schörmann, D. J. As, and K. Lischka, Appl. Phys. Lett. **92**, 201910 (2008).

[19] N. Zainal, S. V. Novikov, C. J. Mellor, C. T. Foxon, and A. J. Kent, Appl. Phys. Lett. **97**, 112102 (2010).

[20] J. Schörmann, S. Potthast, D. J. As, and K. Lischka, Appl. Phys. Lett. **89**, 131910 (2006).

[21] T. Schupp, K. Lischka, and D. J. As, J. Cryst. Growth **312**, 1500 (2010).

[22] O. Brandt, P. Waltereit, and K. H. Ploog, J. Phys. D **35**, 577 (2002).

[23] L. Patrick and W. J. Choyke, Phys. Rev. **123**, 813 (1961).

[24] A. Helman, M. Tchernycheva, A. Lusson, E. Warde, F. H. Julien, K. Moumanis, G. Fishman, E. Monroy, B. Daudin, L. S. Dang, E. Bellet-Amalric, and D. Jalabert, Appl. Phys. Lett. **83**, 5196 (2003).

[25] M. Tchernycheva, L. Nevou, L. Doyennette, F. H. Julien, E. Warde, F. Guillot, E. Monroy, E. Bellet-Amalric, T. Remmele, and M. Albrecht, Phys. Rev. **73**, 125347 (2006).

[26] F. H. Julien, M. Tchernycheva, L. Nevou, L. Doyennette, R. Colombelli, E. Warde, F. Guillot, and E. Monroy, Phys. Status Solidi A **204**, 1987 (2007).

[27] T. Unuma, M. Yoshita, T. Noda, H. Sakaki, and H. Akiyama, J. Appl. Phys. **93**, 1586 (2003).

[28] L. E. Ramos, L. K. Teles, L. M. R. Scolfaro, J. L. P. Castineira, A. L. Rosa, and J. R. Leite, Phys. Rev. B **63**, 165210 (2001).

[29] N. Binggeli, P. Ferrara, and A. Baldereschi, Phys. Rev. B **63**, 245306 (2001).

[30] F. Litimein, B. Bouhafs, Z. Dridi, and P. Ruterana, New J. Phys. **4**, 64 (2002).

[31] M. Helm, in *Intersubband Transition in Quantum Wells: Physics and Device Applications I*, Vol. 62 of *Semiconductors and Semimetals*, edited by H. C. Liu and F. Capasso (Academic, New York, 2000).

[32] C. Q. Chen, R. Helbiga, J. Zemanb, and A. J. L. Poulterb, Physica B **293**, 402 (2001).